

EFFECT OF SOLID AND PERFORATED EXTENSION ON TRAILING EDGE NOISE OF AIRFOIL

Sumesh C. K.

*Research Scholar, Department of Mechanical Engineering, National Institute of Technology Calicut.
email: sumesh55ck@gmail.com*

T. J. Sarvoththamma Jothi

*Department of Mechanical Engineering, National Institute of Technology Calicut, India
e-mail: tjsjothi@nitc.ac.in*

Turbulent boundary layer trailing edge noise is the dominant noise in airfoil self-noise. This noise generated by the trailing edge can be minimised by different edge treatments. By varying the acoustic impedance of the trailing edge acoustic radiation can be varied. A NACA0012 symmetric airfoil with 0.3mm thick solid and perforated plate fitted at the trailing edge is used for this study. Experiments were carried out in an anechoic facility at different velocity varying from 20 m/s to 45 m/s and geometric angles of attack of 0°. Solid trailing edge extension and perforated trailing edge extensions enhance the noise reduction in the low frequency range. As compared to solid extensions perforated extensions provide greater noise reduction. Maximum noise reduction of approximate 6.5 dB in the low frequency range is obtained for the perforate plate attachment at zero angle of attack. At higher velocities an increase in the high frequency noise is observed due to the roughness offered by the perforated extension plate. OASPL analysis shows the strong dependency of the trailing edge with the jet velocity.

Keywords: Perforated extension, noise reduction, finite element methods)

1. Introduction

The increase in air traffic and stringent legislation in the aviation industry invites substantial research attention in abating aircraft noise. One of the major contributors to the aircraft noise is the airframe noise, which is typically generated by the high lift devices and the landing gears particularly at approach conditions. Minimising the noise caused by the turbulent flow past the trailing edge of the high lift devices is remains a challenge. There are various noise generating mechanisms associated with airfoil self-noise[1]. Among these, turbulent boundary layer trailing edge noise is the dominant airfoil self-noise mechanism, which generally happens when turbulent boundary layer is developed over the airfoil. When the vortical structures within the turbulent boundary layer passes the sharp trailing edge of an airfoil, it gets scattered and converted to acoustic waves[2].Trailing edge noise depends on hydrodynamic behaviour of the flow field and the scattering efficiency of the edge. The latter can be minimised by either bevelling or by rounding the trailing edge[3] or by reducing the acoustic impedance of the trailing edge by serrations [4][5][6] and porous treatments[7][8][9].

The idea of reducing flow induced trailing edge noise by varying surface impedance using porous treatment was first proposed by Hayden [7]. Bohn [10] conducted experimental studies in a flat plate to reduce the noise by inserting a porous extension at the trailing edge. The results showed that the maximum noise reduction is observed at a frequency proportional to the ratio of eddy convection velocity to extension length of the porous plate. Revell et al. [11] studied experimentally the effect of porous treatment on reducing the noise generated due to the interaction of the side edge rolled vortex with the flap. Treating the side edge of the flap with porous material significantly reduces the radiated noise. Many biological studies on the quiet flight of owl reveals that the porosity and/or permeability is one of the dominant features of an owl's wing which helps in its quieter flight [12,13]. Further studies on the noise reduction capability of owl's wing were conducted by Bachmann et al. [14] and they concluded that the greater porosity of the owl's feather compared to that of pigeon, enhances the airflow from the wing pressure side to the suction side helps in its quiet flight.

Geyer et al. [15] conducted a comprehensive study on the factors affecting the noise generated by a porous airfoil. The air flow resistivity and the surface roughness of the material decides the noise reduction attained by the porous treatment. Through the experiments they showed that in the low and moderate frequency range up to 10 kHz, a noise reduction up to 10 dB can be attained by the porous airfoil than that of non-porous airfoil. However, a noise increase is observed above 10kHz attributed by the surface roughness of the porous coating. The experiments conducted by Herr et al. [9] on the flow-permeable trailing edges also revealed the effectiveness of flow permeable materials in trailing edge noise abatement. They have reported that the brush edge extensions have significant edge noise reduction potential varying from 2 to 14 dB. They hypothesized that the viscous damping of turbulent flow pressure fluctuations in the trailing edge brush area cause the noise reduction

Angland et al. [16] conducted an experimental study to understand the effect of porous treatment on the flap side-edge in noise reduction using PIV and surface pressure measurements. The reduction in the noise generated by the airframe is obtained due to the displacement of the vortices away from the airfoil surface by altering the formation of shear layer near the airfoil side edge due to the presence of porous side edge. This in turn changes the pressure distribution over the surface and thus causes change in acoustic impedance which leads to the noise reduction.

The present work describes preliminary results of the experiments conducted to study the effect of solid and perforated trailing edge extensions on the flow induced noise reduction of a symmetric airfoil. The focus of the study is limited to trailing edge noise as one of the main noise sources on many airfoil applications. The intention of the study is to understand the influence of perforation provided on the add-on trailing edge extensions of an airfoil.

2. Methodology

2.1 Experimental Facility and Test model

The acoustic measurements were carried out in an open jet wind tunnel anechoic facility of size 2.5 × 2.5 × 2.5 m having a cut off frequency 300Hz. Air is supplied to the test section by a centrifugal blower driven by a 10HP motor, through an acoustically treated duct and a matched cubic contoured rectangular nozzle with exit cross section 0.2 m x 0.08 m. The maximum flow velocity of the free stream jet is 47 m/s and the measured turbulence intensity at the potential core at maximum jet velocity was estimated to be less than 0.2%, while the background noise is kept low.

A NACA0012 airfoil with chord (c) 0.15 m and span of 0.3m is used for the present study. The airfoil model is immersed in the flow at zero angle of attack in between two side plates attached to the nozzle as shown in Fig.1. These side plates ensure that the flow over the airfoil is two dimensional. Moreover, since the span of the airfoil is more than the nozzle width, the side plate is away from the nozzle vertical

side and which prevents the development of the turbulent boundary layer along the side plate. This reduces the background noise level as well as the contamination by the leading-edge noise[17,18]. In order to examine the interaction of a turbulent boundary layer with trailing edge, eradication of laminar boundary layer development on the airfoil surface is essential. The turbulent boundary layer over the airfoil on both sides are artificially generated by pasting a strip of sandpaper of 80-grit size and width 0.01m on both sides of the airfoil at a distance 0.03m (0.2c) downstream of the leading edge.

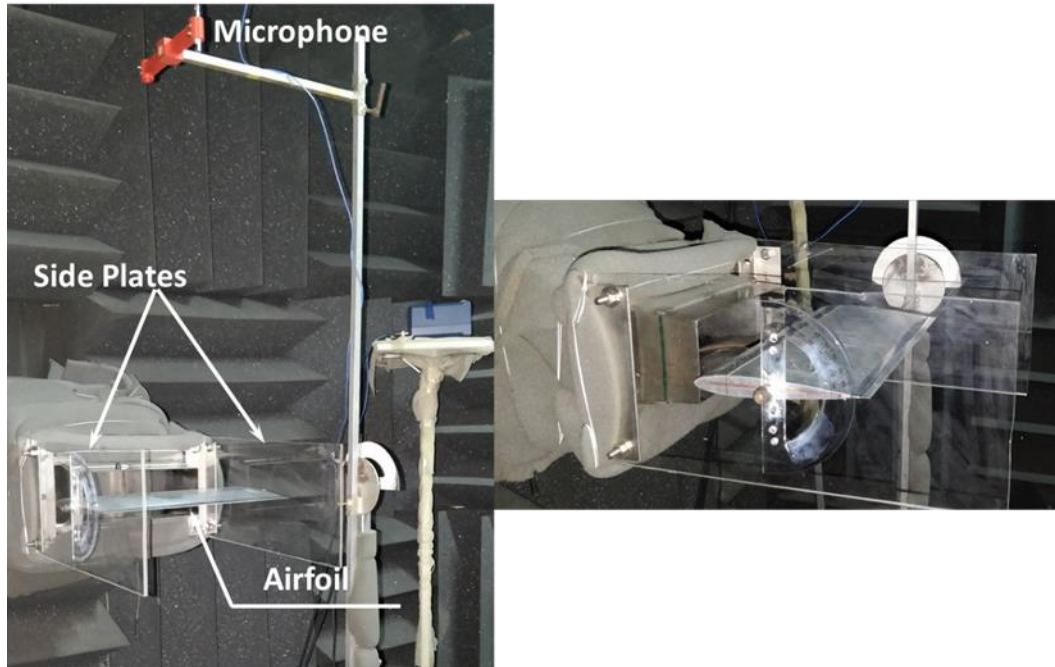


Figure:1 Experimental setup with airfoil held between the side plates

The airfoil is placed in front of the nozzle such that the leading edge of the airfoil is at a distance of 25mm from the nozzle exit plane to minimize the turbulence interaction noise of the leading edge as shown in Fig. 1. The interaction of shear layers created at the nozzle lips with the trailing edge would have potential impact on the trailing edge noise. The nozzle width decides the extent of the potential core of the jet and is generally assumed to be four to five times of the jet widths. Thus, it is confirmed that the airfoil is placed within the potential core of the jet.

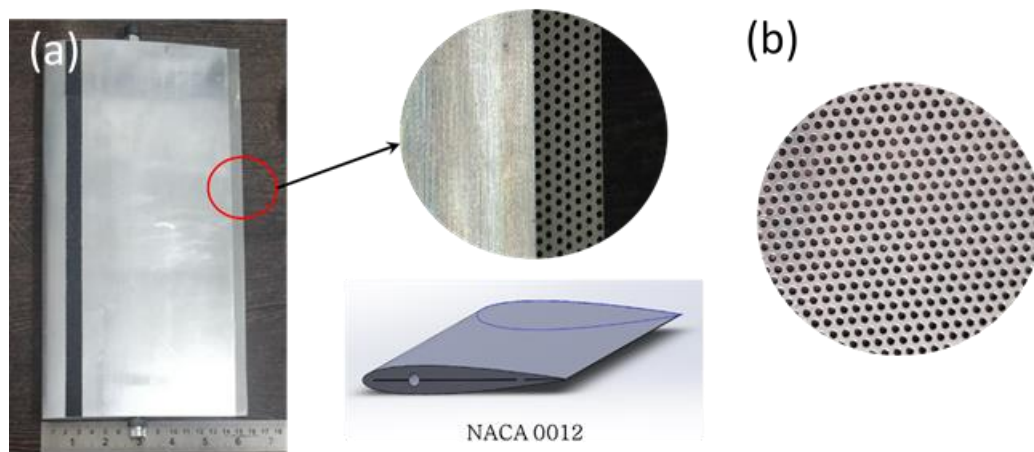


Figure:2 (a) Airfoil test model with trailing edge extension (b) Close view of Perforated extension

A solid and perforated extension plates of length 10mm and having a thickness of 0.3 mm were used to study the difference in noise characteristics of the trailing edge. In order to attach the solid and perforated plate extension to the airfoil a 0.5 mm slit is made along the span of the airfoil as shown in Fig. 2. The perforated plate is having mesh size 18 with hole diameter 430 μm . The jet velocities under considerations for this experiment are between 20 m/s to 45m/s and corresponding Reynolds Numbers based on the chord length varies from 1.89×10^5 to 4.3×10^5 .

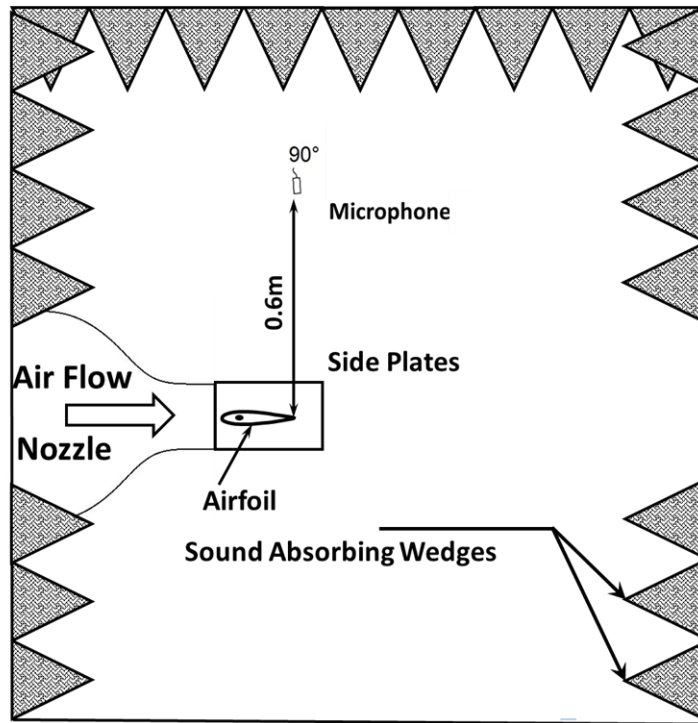


Figure 3: Schematic of the for the acoustic measurement setup.

2.2 Acoustic Measurements and data processing

The Fig. 3 shows the schematic of the experimental set up for the acoustic measurements. As shown in Fig. 3, the far field noise measurements were taken by a single $\frac{1}{4}$ " PCB (PCB - 378C01) made condenser microphone at a distance of 0.6m above the mid span of the aerofoil trailing edge at polar angles of 90^0 . The output voltage signals from the microphone were first passed on to a PCB signal conditioner then to a National Instruments PCI- 6143 DAQ card through NI BNC-2110 noise Rejecting, shielded BNC Connector Block. The noise data was acquired at a sampling frequency of 150 kHz and for a duration of 16s as successive samples of duration of 2s. These five sets of two second data are then combined to form a 10s data. This time domain noise data is then converted to frequency domain using *pwelch* function with 2^{13} point FFT with hanning window function and 50% overlap. The frequency resolution of the resulting spectrum is 18.31 Hz.

3. Experimental Results and Discussion

This section describes the noise reduction potential of the solid and perforated extensions on trailing edge noise, measured in an anechoic environment under free field condition. Fig. 4 represents the background corrected far field acoustic Power Spectral Density (PSD) spectrum of the base trailing edge, solid extension and perforated extension at different velocities. The figure demonstrates that the add-on extension to the trailing edge has substantial effect on the Power Spectral Density spectra. Both solid and perforated extension shows reduction in noise levels. Noise reduction for the solid trailing edge extension is less as compared to the perforated extension. The noise radiated from the solid trailing edge extension is more or less same as compared to that of base trailing edge at velocities 35 and 40 m/s and shows a reduction in noise levels at 45 m/s. However, appreciable noise reduction is obtained in the case of perforated trailing edge extension within the frequency range 3.3kHz.

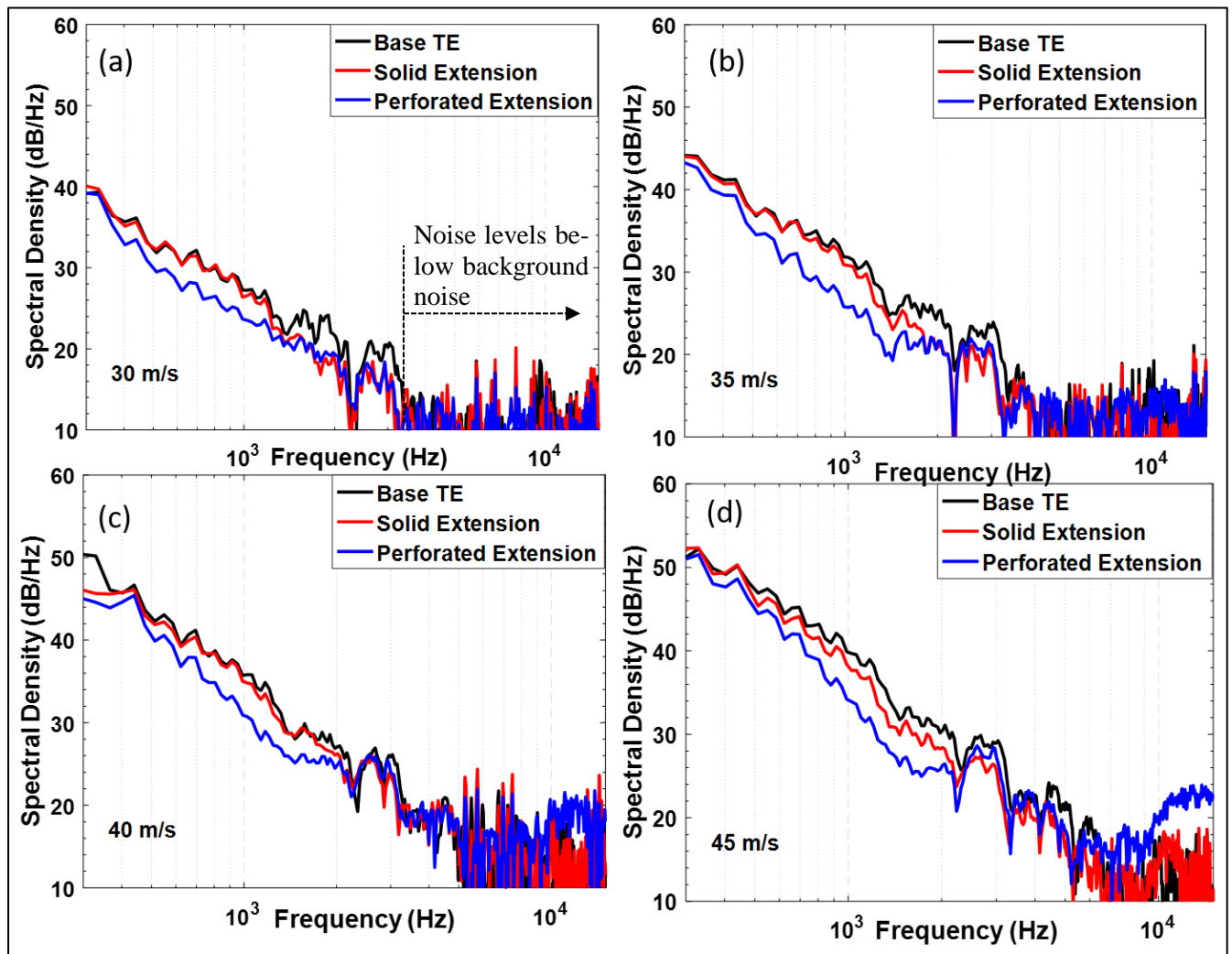


Figure 4. Spectral comparison of airfoils with trailing edge extensions at $\alpha = 0^\circ$ (a) $U_\infty = 30$ m/s (b) $U_\infty = 35$ m/s (c) $U_\infty = 40$ m/s (d) $U_\infty = 45$ m/s

In Fig.4(c) and (d) above 8 kHz a broadband hump can be seen which is slightly above the noise generated by the other two cases. This increase in the noise levels are attributed by the roughness offered by the extension plate.

In order to quantify the noise reduction at different frequencies the difference in the Sound Pressure Levels between the base trailing edge and perforated trailing edge was calculated using equation 1.

$$\Delta SPL = SPL_{base} - SPL_{TE\ extension}. \quad (1)$$

The positive values of ΔSPL represents the reduction in SPL and negative values indicates increase in SPL. Figures 5(a) & 5(b) displays the contour colour maps of ΔSPL as a function of free stream velocity and frequency for the solid trailing edge extension and perforated trailing edge extension respectively. The colour map is plotted in the same range of colours. Appreciable reduction in the noise levels have been attained by perforating the trailing edge extension. By comparing figures 5(a) it is evident that, for solid trailing edge extension, a noise reduction of less than 2dB is attained in the frequency range below 1.3 kHz and maximum 4.6 dB reduction at frequency 1.6 kHz at velocities below 30m/s. At velocities greater that 30 m/s maximum of 3dB reduction is attained below 3.3kHz. The level of noise reduction is found to be negative at frequencies above 3.3kHz, which indicates that the noise levels increase as compared to base trailing edge. Fig.5(b) represents the noise reduction level (ΔSPL) of perforated trailing edge extension. It is evident from the Fig.5(b) that, at low frequencies approximately below 3.3kHz the reduction in noise levels of perforated extension is greater than that of solid extension. Approximately 6.5dB reduction can be attained at the maximum velocity under consideration. However, at frequencies greater than 3.3kHz, ΔSPL shows negative values which implies an increase in noise levels as compared to the base trailing edge. The hike in noise levels in the high frequency region, especially at high velocities is attributed by the roughness offered by the perforated extension plate. The increase in the noise due to the roughness is in congruence with the results reported by Geyer et al. [15]

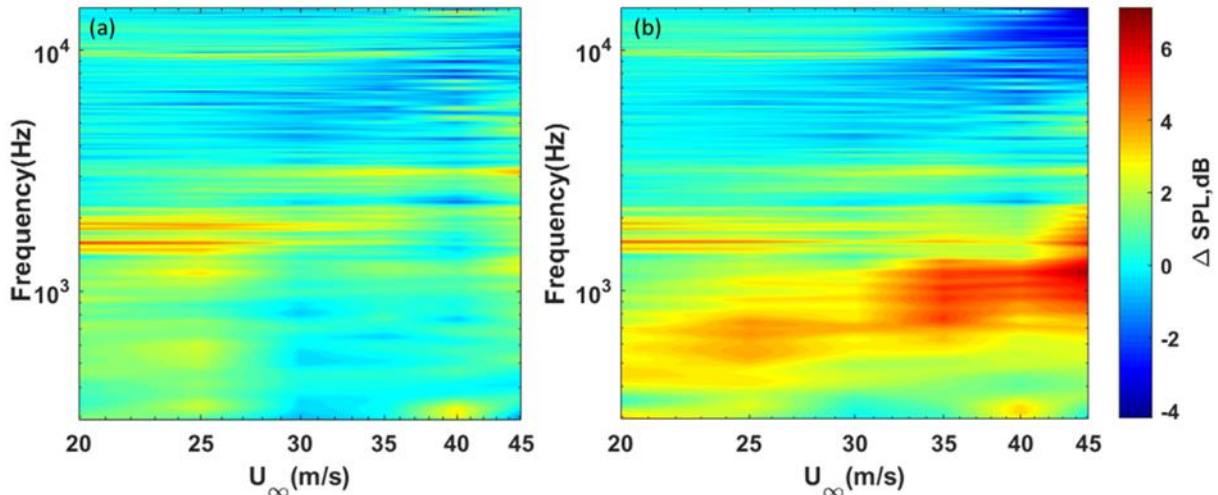


Figure 5. Colour map of ΔSPL (a) Solid TE extension (b) Perforated TE extension

From the above discussion it is clear that the add-on trailing edge extension brings a reduction in the low frequency trailing edge noise and an increase in high frequency noise as compared to the base trailing edge. So it is important to examine the overall effect in the noise abatement. To study the overall effect, the overall sound pressure level (OASPL) of the trailing edge noise at a particular velocity is calculated for both trailing edge extensions along with the base trailing edge. The OASPL for the narrow band frequency spectra is calculated by integrating the sound pressure level SPL_i corresponding to the narrow frequency within the range of 300 Hz to 15 kHz. The lower limit of frequency chosen as the cut-off frequency of the anechoic chamber.

$$OASPL = 10 \cdot \log_{10} \left(\sum_i 10^{\left(\frac{SPL_i}{10}\right)} \right) dB \quad (2)$$

Where SPL_i is the sound pressure level at the i^{th} narrow band frequency.

Figure 6 represents the dependency of OASPL of the trailing edge noise as on the flow speed at zero angle of incidence. For both trailing edge extensions and base trailing edge, the overall sound pressure level increases with flow velocity. A little difference can be seen in the OASPL levels of base trailing edge and solid trailing edge extension. The OASPL of for the base trailing edge is slightly greater than that of the solid trailing extension remains nearly constant in the velocity range 0–40 m/s and the opposite effect can be seen at velocity 45m/s. However, significant reduction in the OASPL level can be observed in the case of perforated trailing edge extension. Even though the OASPL levels increase with flow velocity in all cases, the perforated trailing edge extension shows a different slope. The OASPL levels of base trailing edge and solid trailing edge extension varies approximately with a velocity dependence of $OASPL \propto U_\infty^5$ for all the velocities under consideration. The increase in OASPL with velocity for the perforated trailing edge extension scales with the power law $OASPL \propto U_\infty^{4.6}$. This implies that the noise radiated from the perforated extension has a strong dependence on the free stream velocities compared to the other two. Also, these values of the power law indices (5 and 4.6) show good agreement with the experiments of Brooks et al. [1] and Howe [19]. This also confirm that the dominant noise mechanism is the acoustic radiation from the trailing edge which is well above the background noise and isolated from the other noise source such as leading-edge noise.

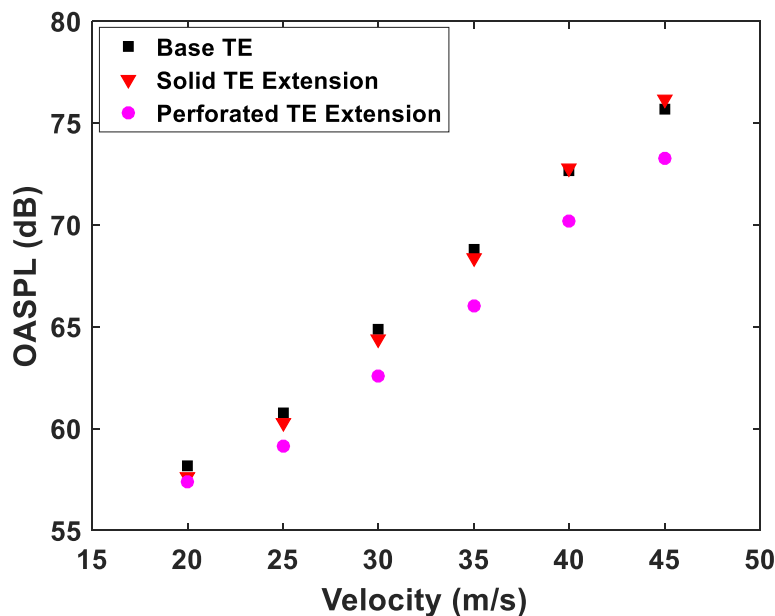


Figure 6: Variation of OASPL with flow speed

4. Conclusion

This paper presented the comparison of noise reduction characteristics of a solid and perforated trailing edge extensions retrofitted on a NACA0012 airfoil. The acoustic data were measured experimentally at different flow velocities at zero angle of incidence. It is observed that a perforated extension is more effective than a solid extension and a noise reduction up to 6.5dB were noticed for the perforated extension at low and medium frequencies. This implies that the noise reduction depends on the permeability of the trailing edge extension. At high frequencies, the perforated trailing edge extension cause more noise than the base trailing edge, which might be due to the surface roughness noise. The OASPL analysis

reveals that overall noise levels strongly depends on the flow velocity and the noise perforated trailing edge scales with 4.6 power of velocity while the solid and perforated extension scales with a power of 5.

Acknowledgement

The authors gratefully acknowledge the research funding from the Department of Science and Technology (DST) – Science and Engineering Research Board (SERB) vide Project No. SB/FTP/ETA-0137/2013.

REFERENCES

- 1 Brooks, T. F., Pope, D. S., and Marcolini, M. A., Airfoil Self-Noise and Prediction," NASA RP-1218, 1989.
- 2 M. Roger and S. Moreau, "Trailing Edge Noise Measurements and Prediction for Subsonic Loaded Fan Blades," AIAA Pap., no. June, pp. 2460–2460, 2002.
- 3 M. S. Howe, "The Influence of Surface Rounding on trailing edge noise," J. Sound Vib., vol. 126, no. 3, pp. 503–523, 1988.
- 4 M. S. Howe, "Noise produced by a sawtooth trailing edge," J. Acoust. Soc. Am., vol. 90, no. 1, pp. 482–487, 1991.
- 5 M. Gruber, P. Joseph, and T. Chong, "On the mechanisms of serrated airfoil trailing edge noise reduction," 17th AIAA/CEAS Aeroacoustics Conf. (32nd AIAA Aeroacoustics Conf., no. June, pp. 5–8, 2011.
- 6 C. Arce León, D. Ragni, S. Pröbsting, F. Scarano, and J. Madsen, "Flow topology and acoustic emissions of trailing edge serrations at incidence," Exp. Fluids, vol. 57, no. 5, pp. 1–17, 2016.
- 7 R. E. Hayden, "Fundamental aspects of noise reduction from Powered-Lift devices," SAE Trans., pp. 1287–1306, 1973.
- 8 T. Geyer, E. Sarradj, and C. Fritzsche, "Porous airfoils: noise reduction and boundary layer effects," Int. J. Aeroacoustics, vol. 9, no. 6, pp. 787–834, 2010.
- 9 M. Herr and W. Dobrzynski, "Experimental Investigations in Low-Noise Trailing-Edge Design," AIAA J., vol. 46, no. 6, pp. 1167–1175, 2005.
- 10 A. J. Bohn, Edge Noise Attenuation by Porous-Edge Extensions, AIAA J.,76, 1976 0–8.
- 11 Revell, J. D., Kuntz, H. L., Balena, F., Horne, W. C., Storms, B. L., and Dougherty, R. Trailing edge ap noise reduction by porous acoustic treatment. 3rd AIAA/CEAS Aeroacoustics Conference, AIAA paper, 97-1646 1997
- 12 Kroeger RA, Gruschka HD, Helvey TC, Low speed aerodynamics for ultra-quiet flight. AFFDL TR 971-75,1971
- 13 Lilley G M , A study of the silent flight of the owl, AIAA Paper 1998-2340.
- 14 T. Bachmann, S. Klän, W. Baumgartner, M. Klaas, W. Schröder, and H. Wagner, "Morphometric characterisation of wing feathers of the barn owl *Tyto alba pratincola* and the pigeon *Columba livia*," Front. Zool., vol. 4, pp. 1–15, 2007.
- 15 T. Geyer, E. Sarradj, and C. Fritzsche, "Measurement of the noise generation at the trailing edge of porous airfoils," *Exp. Fluids*, vol. 48, no. 2, pp. 291–308, 2010.
- 16 D. Angland, X. Zhang, and N. Molin, "Measurements of Flow Around a Flap Side Edge with Porous Edge Treatment," AIAA J., vol. 47, no. 7, pp. 1660–1671, 2009.
- 17 D. J. Moreau, L. A. Brooks, and C. J. Doolan, "Broadband trailing edge noise from a sharp-edged strut," J. Acoust. Soc. Am., vol. 129, no. 5, pp. 2820–2829, 2011.
- 18 D. J. Moreau, M. R. Tetlow, L. A. Brooks, and C. J. Doolan, "Acoustic analysis of flat plate trailing edge noise," Proc. 20th Int. Congr. Acoust., no. August, pp. 1–8, 2010.
- 19 M. S. Howe. A review of the theory of trailing edge noise. Journal of Sound and Vibration, 61:437-465,1978